

TIME DOMAIN ANALYSIS OF HELMHOLTZ SOLITON PROPAGATION USING THE TLM METHOD

P. CHAMORRO-POSADA

*Departamento de Teoría de la Señal y Comunicaciones e Ingeniería Telemática,
Universidad de Valladolid, ETSI Telecomunicación,
Paseo Belén 15, E-47011 Valladolid, Spain
pedcha@tel.uva.es*

G. S. McDONALD

*Joule Physics Laboratory, Materials and Physics Research,
School of Computing, Science and Engineering,
University of Salford, Salford M5 4WT, United Kingdom*

Received 15 August 2012

The transmission line matrix method is used to study Helmholtz solitons as solutions of the two-dimensional time-domain Maxwell equations in nonlinear media. This approach permits to address, in particular, the propagation and intrinsic stability properties of subwavelength soliton solutions of the scalar nonlinear wave equation and the behavior of optical solitons at arbitrary interfaces. Various numerical issues related to the analysis of soliton beams using the time-domain method are also discussed.

Keywords: Helmholtz solitons; TLM method; subwavelength solitons.

1. Introduction

The two-dimensional (2D) nonlinear scalar wave (SW) equation is conventionally used for the study of soliton light beams. This equation describes exactly the nonlinear evolution of pure 2D transverse electric (TE) electromagnetic fields, but it is also a very good theoretical framework for most common planar experimental setups.¹ For continuous-wave (CW) beams under paraxial propagation conditions, the nonlinear SW equation reduces to the nonlinear Schrödinger (NLS) equation that is a standard mold for the analysis of spatial optical solitons.² The NLS equation can be integrated analytically,² for a certain class of material responses, or numerically, using highly efficient algorithms.³

If paraxial propagation is not assumed, the scalar nonlinear Helmholtz (NLH) equation is obtained from the SW equation in the CW case without the resource of any approximation. The NLH framework allows to study optical solitons under

P. Chamorro-Posada & G. S. McDonald

arbitrary *angular* nonparaxial conditions.⁴⁻⁶ A class of numerical algorithms⁷ has been put forward for the effective computational solution of this nonintegrable⁸ nonlinear evolution equation and has permitted to assess the robustness of the exact Helmholtz soliton solutions in a range of nonlinear optical materials⁹⁻¹⁴ and to unveil new effects of soliton propagation and in their interaction with interfaces.^{8,15-18}

In spite of the effectiveness of the nonparaxial beam propagation method⁶ (NPBPM) for the solution of such a broad range of problems, it is not absolutely free of limitations. Since the NLH equation is of second-order in the evolution coordinate, those components of the angular spectrum corresponding to evanescent waves must be filtered out as part of the propagation algorithm. Otherwise, they would show up in the solution as exponentially growing signals.⁶ The filtering incorporated in the numerical algorithm restricts the situations that can be studied to those where deviations of the total (linear and nonlinear) refractive index relative to that of a reference value are very small. Therefore, only small intensity beams with very modest self-induced nonlinear contribution to the refractive index can be considered. This type of optical signals corresponds, precisely, to those properly described by SW equation and define a type of (angular) Helmholtz nonparaxiality. An archetypal Helmholtz nonparaxial problem is that of the behavior of optical solitons at the planar boundary between two nonlinear media.¹⁵⁻¹⁸ Notwithstanding the wealth of the new interface phenomena that have been uncovered using Helmholtz theory, the numerical studies based on the NPBPM are limited to very small relative differences in the linear and nonlinear refractive indexes.

In this work, we use the transmission-line matrix (TLM) method¹⁹⁻²¹ for the study of the solitons of the scalar NLH equation solving the 2D time-domain Maxwell equations in CW case. We show that this approach permits to investigate the behavior of optical solitons at arbitrary optical interfaces and also allow us to extend our analyses to the *high-intensity* nonparaxial regime. In particular, subwavelength soliton solutions of the NLH equation are known to exist,²² in spite of the fact that they are not expected to represent a solution physically feasible in a straightforward manner. These solutions belong to the family of the Helmholtz solitons⁴ when this is extended to the ultra-narrow regime. Notwithstanding, in any realistic scenario, neither scalar nor reasonably true 2D propagation can be assumed under such strong nonlinear propagation conditions capable of raising polarization and high-order nonlinear effects, but the issues of the existence and the stability of scalar subwavelength solitons are still of theoretical interest and they have been the subject of discussion in the scientific literature.^{22,23} The use of the time-domain Maxwell equations also opens other possibilities for the extension of previous studies, for instance, by the inclusion of the temporal dynamics.

Even though beam propagation methods³ combining high numerical accuracy and computational effectiveness have largely dominated the numerical studies on optical solitons, the steady increase of the available computing power has opened

the numerical investigations to time-domain integrators of the nonlinear Maxwell equations over the last decade. The finite-difference time-domain (FDTD) method is the most common alternative and it has been employed in the study of the propagation of light bullets,²⁴ the interaction of soliton beams²⁵ or the interaction of ultra-narrow solitons with left-handed surfaces.²⁶ Nevertheless, the FDTD is not the only tool for the time-domain integration of Maxwell equations; for instance, direct integrators²⁷ have also been used.

The TLM method was first introduced by Johns and Beurle¹⁹ and has been applied mostly in the fields of radio frequency and power systems but also in acoustics and diffusion problems.²¹ In Ref. 28 it was used for the analysis of 2D linear photonic devices. Even though TLM and FDTD display similar performance properties, the TLM method still holds conceptual advantages that make it specially appealing. Instead of producing a discrete approximate numerical representation for the physical dynamics as in the FDTD method, the formulation of the TLM method creates an approximate physical model for the physical system we want to analyze. This model is then solved exactly. Also, the TLM formulation of linear passive propagation problems is subject to the laws of conservation of charge and energy and, therefore, is unconditionally stable. This stability, based on physical grounds, can be preserved in a judicious formulation of the TLM algorithm for the propagation in nonlinear media.

2. 2D Maxwell Equations and the NLH Equation

We consider the 2D propagation of a light field as described by the full Maxwell equations. In a pure 2D scenario the spatial variations along one particular coordinate (y , in our case) are null, $\partial_y = 0$, and Maxwell equations decouple into two independent systems of equations that have attached two corresponding types of solutions that evolve in the xz propagation plane. The transverse magnetic (TM) solutions have an electric field intensity lying on the propagation plane whereas the magnetic field intensity is polarized in the y direction. In the TE solution, the polarization properties of the electric and magnetic fields are reversed.

We focus here on the TE problem with $\mathbf{E}(x, z, t) = \hat{\mathbf{y}}E_y(x, z, t)$ for which Maxwell equations in a nonmagnetic medium are

$$\frac{\partial E_y(x, z, t)}{\partial x} = -\mu_0 \frac{\partial H_z(x, z, t)}{\partial t}, \quad (2.1)$$

$$\frac{\partial E_y(x, z, t)}{\partial z} = \mu_0 \frac{\partial H_x(x, z, t)}{\partial t} \quad \text{and} \quad (2.2)$$

$$\frac{\partial H_x(x, z, t)}{\partial z} - \frac{\partial H_z(x, z, t)}{\partial x} = \epsilon_0 n^2(x, y) \frac{\partial E_y(x, z, t)}{\partial t}, \quad (2.3)$$

where $\mu_0 = 4\pi \times 10^{-7}$ H/m is the magnetic permeability, $\epsilon_0 = (\mu_0 c^2)^{-1}$ F/m is the vacuum permittivity and n the refractive index. If we take the x derivative in (2.1),

P. Chamorro-Posada & G. S. McDonald

the z derivative in (2.2) and the time derivative in (2.3), upon substitution of the results of (2.1) and (2.2) in (2.3), the wave equation

$$\frac{\partial^2 E_y(x, z, t)}{\partial x^2} + \frac{\partial^2 E_y(x, z, t)}{\partial z^2} - \mu_0 \epsilon_0 n^2(x, y) \frac{\partial^2 E_y(x, z, t)}{\partial t^2} = 0, \quad (2.4)$$

is obtained.

In the time-harmonic CW case, the spatial evolution of the electric field intensity is described by the complex field $\tilde{E}(x, z)$ with $E_y(x, z, t) = \Re\{\tilde{E}(x, z) \exp(-i\omega_0 t)\}$. When this expression is substituted into (2.4), one obtains the Helmholtz equation

$$\frac{\partial^2 \tilde{E}(x, z)}{\partial x^2} + \frac{\partial^2 \tilde{E}(x, z)}{\partial z^2} + \frac{\omega_0^2 n^2(x, y)}{c^2} \tilde{E}(x, z) = 0, \quad (2.5)$$

where nonlinearity is brought into the evolution equation through the relation

$$n^2 = n_0^2 + n_{\text{NL}}^2(E). \quad (2.6)$$

If the nonlinear contribution to the refractive index is assumed to be $n_{\text{NL}}^2 = 2n_0 n_2 |\tilde{E}|^2$ (where n_0 is the linear refractive index and n_2 the Kerr coefficient) and the complex electric field intensity is written in terms of a normalized complex envelope $u(x, z)$ as $\tilde{E}(x, z) = \sqrt{I} u(x, z) \exp(ikz)$, where $I = (kn_2 L_D / n_0)^{-1}$ and $k = (\omega_0 / c) n_0 = 2\pi / \lambda$, one obtains the nonparaxial nonlinear Schrödinger (NNLS) equation⁴

$$\kappa \frac{\partial^2 u(\xi, \zeta)}{\partial \zeta^2} + i \frac{\partial u(\xi, \zeta)}{\partial \zeta} + \frac{1}{2} \frac{\partial^2 u(\xi, \zeta)}{\partial \xi^2} + |u(\xi, \zeta)|^2 u(\xi, \zeta) = 0, \quad (2.7)$$

where $\zeta = z / L_D$, $\xi = \sqrt{2}x / w_0$ and $L_D = kw_0^2 / 2$ is the diffraction length of a reference Gaussian beam with waist w_0 . The nonparaxiality parameter

$$\kappa = \frac{1}{(kw_0)^2} = \frac{1}{4\pi^2} \left(\frac{\lambda}{w_0} \right)^2, \quad (2.8)$$

is proportional to the square inverse of the ratio of the beam waist to the optical wavelength $\lambda = \lambda_0 / n_0$ of a linear optical signal in the medium. The normalized equations (2.7) can be alternatively obtained from (2.5) using the characteristic length scale of the nonlinear effects $L_{\text{NL}} = \lambda_0 / (2\pi n_2 I)$, instead of the diffraction length L_D as a reference. Using the scaling $\zeta = z / L_{\text{NL}}$, (2.7) and (2.10) are obtained from (2.5). The nonparaxiality parameter in this alternative (equivalent^a) derivation is proportional to the ratio of the nonlinear contribution to the dielectric permittivity to its linear part

$$\kappa = \frac{1}{4} \frac{2n_0 n_2 I}{n_0^2} = \frac{1}{4} \frac{n_{\text{NL}}^2}{n_0^2}. \quad (2.9)$$

^aIn the first derivation, which leads to (2.8), the soliton width is used to normalize the propagation coordinate, L_D . The reference peak amplitude of the solution is then set such that $L_{\text{NL}} = L_D$. In the second derivation that yields (2.9) the z coordinate is first scaled with L_{NL} and the normalization of the transverse coordinate is then chosen so $L_D = L_{\text{NL}}$. Therefore, both scalings, as well as conditions (2.8) and (2.9), are fully equivalent.

The envelope equation (2.7) is more convenient for the comparison of full Helmholtz results with those obtained from the paraxial NLS equation that is obtained from (2.7) when the first term $\kappa \partial_{\zeta} u$ is neglected. Rescaling the z coordinate according to the x coordinate and reintroducing the fast reference phase permits to recover a scaled version of the NLH equation⁸

$$\frac{\partial^2 U(\xi, \zeta)}{\partial \zeta^2} + \frac{\partial^2 U(\xi, \zeta)}{\partial \xi^2} + \frac{1}{2\kappa} U + 2|U(\xi, \zeta)|^2 U(\xi, \zeta) = 0. \quad (2.10)$$

The exact Kerr bright Helmholtz soliton^{4,6} in this frame has the expression⁸

$$U(\xi, \zeta) = \eta \operatorname{sech} [\eta (\xi \cos \theta + \zeta \sin \theta)] \exp \left[i \sqrt{\frac{1 + 2\kappa\eta^2}{2\kappa}} (-\xi \sin \theta + \zeta \cos \theta) \right], \quad (2.11)$$

where the rotational invariance^{4,6} of the NLH equation solutions is evident.

There is no approximation in going from Eq. (2.5) to (2.7), and both equations are fully equivalent.

3. The 2D TLM Shunt Model

In the 2D shunt-connected TLM formulation a periodic mesh of transmission line sections is deployed over the propagation plane, as shown in Fig. 1. A $\Delta l \times \Delta l$ unit cell of this periodic array is highlighted in the upper left corner of this figure. The electromagnetic properties of each transmission line section are defined by its characteristic impedance Z_0 and propagation velocity u which are related to, but *distinct* from, the wave impedance and velocity in the 2D medium that is being modelled. These magnitudes are equivalently defined by the capacitance and inductance per unit length of the transmission line, C_d and L_d , respectively.

This setup provides a frame that supports the propagation of transmission line voltage and current waves (defined in Fig. 2) that model the electromagnetic magnitudes in the original problem. The correspondence between the transmission line fields (voltages at the mesh nodes and the currents in the transmission line sections) and the electric and magnetic field intensities, respectively, is²¹

$$E_y \leftrightarrow -\frac{V_y}{\Delta l}, \quad (3.1)$$

$$H_x \leftrightarrow \frac{I_z}{\Delta l} \quad \text{and} \quad (3.2)$$

$$H_z \leftrightarrow -\frac{I_x}{\Delta l}. \quad (3.3)$$

Using the equivalent lumped circuit element representation of the transmission line sections of length Δl at a node and the equivalences (3.3), it is immediate to derive the 2D Maxwell equations (2.1)–(2.3) from the TLM model^{19,21} in the limit $\Delta l \rightarrow 0$.

P. Chamorro-Posada & G. S. McDonald

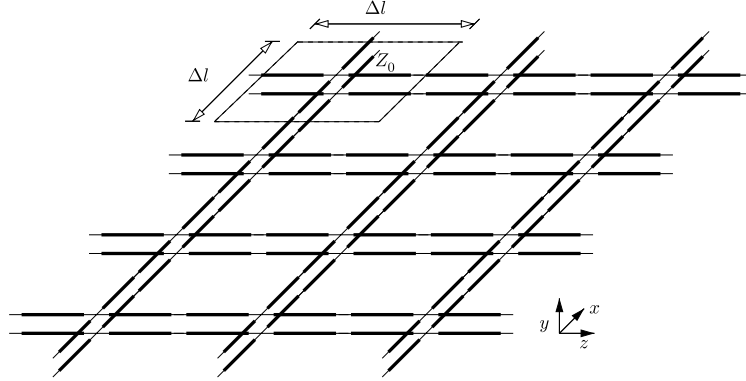


Fig. 1. Schematic illustration of the 2D shunt-connected TLM mesh.

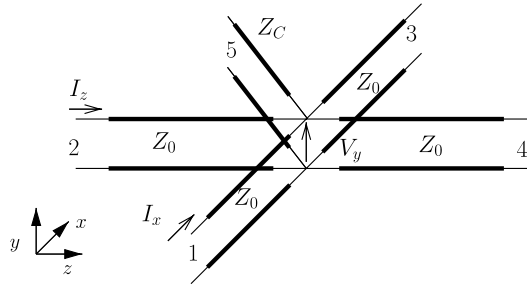


Fig. 2. Schematic representation of a shunt TLM node with a capacitive stub.

A change in the linear refractive index can be modelled through a capacitive stub. The contribution of the polarization current in the propagation medium to the total displacement current is represented by the current at the input of a short open-ended transmission line section with characteristic impedance Z_C , as shown in Fig. 2. The length of the stub and its propagation velocity must be chosen in such a way that the synchronism of all the signals in the TLM mesh is preserved. The full correspondence with the medium parameters is, then, given by

$$\mu_0 \leftrightarrow Z_0 \frac{\Delta t}{\Delta l}, \quad (3.4)$$

$$\epsilon_0 n_0^2 \leftrightarrow \frac{2\Delta t}{Z_0 \Delta l} \left(1 + \frac{Z_0}{4Z_C} \right). \quad (3.5)$$

Figure 2 depicts a node in the TLM mesh, where five transmission line sections are shunt connected. At time $t = k\Delta t$, $V_{i,l}^{(k)}$ is the wave propagating along transmission line l towards the node. The five incident components are then scattered producing the reflected components $V_{r,l}^{(k)}$ which, at the next iteration of the

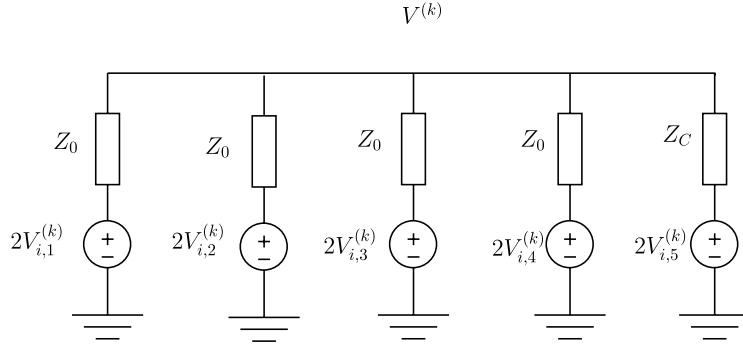


Fig. 3. Equivalent circuit for the TLM shunt node.

algorithm, become the incident components at adjacent nodes after a transmission delay Δt . The scattered components can be calculated from the incident components at each line and the node voltage V^k at $t = k\Delta t$ which is readily obtained from the node equivalent circuit shown in Fig. 3. The resulting scattering matrix is

$$\mathbf{S} = \frac{1}{\hat{Y}} \begin{bmatrix} 2 - \hat{Y} & 2 & 2 & 2 & 2\hat{Y}_C \\ 2 & 2 - \hat{Y} & 2 & 2 & 2\hat{Y}_C \\ 2 & 2 & 2 - \hat{Y} & 2 & 2\hat{Y}_C \\ 2 & 2 & 2 & 2 - \hat{Y} & 2\hat{Y}_C \\ 2 & 2 & 2 & 2 & 2\hat{Y}_C - \hat{Y} \end{bmatrix}, \quad (3.6)$$

where $\hat{Y}_C = Z_0/Z_C$ and $\hat{Y} = 4 + \hat{Y}_C$.

A nonlinear contribution to the displacement current during the propagation can be incorporated by loading the TLM node with a nonlinear capacitive element. Since the early works of Johns and O'Brien,²⁹ many proposals for the incorporation of nonlinear reactive elements in TLM models using either link or stub transmission line sections have been put forward.^{30–35} In Ref. 30, several early approaches are analyzed and one stub model with impedance varying over the time step is proposed. In this scheme,³⁰ the characteristic impedance of the capacitive stub modelling the nonlinear dielectric susceptance is itself a nonlinear function of the signal propagating along it. This configuration permits the conservation of the charge and energy in the nonlinear TLM formulation. In the approach introduced in Ref. 35, a change in the refractive index is modelled by the sudden switch of a capacitive stub with no initial incident voltage.

Most nonlinear TLM models result in implicit schemes that require to solve a nonlinear equation at each node for each time instant. This task can be efficiently accomplished by the use of the Newton–Raphson algorithm which typically converges in a very small number of iterations or using the direct solution of the third-order equation. Several schemes have been tested by us rendering essentially

P. Chamorro-Posada & G. S. McDonald

equivalent results. For the numerical simulations, we have used an efficient parallel implementation of the algorithm using the parallel virtual machine (PVM) as message passing library.

4. Results and Discussion

The nonparaxiality parameter κ , as given by (2.8), becomes larger as the width of the exact Helmholtz soliton (2.11) solution approaches the size of the wavelength. Such a decrease of the soliton width, in turn, requires a stronger relative contribution of the nonlinear self-induced component to the total refractive index that can be read from (2.9). In this regime of strong nonlinearity, the nonlinear parametric processes in the medium are significantly enhanced. Even though the propagation of a signal in the TLM mesh is subject to some (normal) dispersion of numerical origin,^{19,21} this dispersion can be very small for very fine spatial discretizations. This means that the conversion to the third harmonic through four wave mixing (FWM) effects in the presence of a instantaneous nonlinearity $n_{\text{NL}}^2 = \alpha E_z(x, z, t)^2$ can be very strong. Third harmonic generation (THG) may act as a perturbation that hinders an accurate representation of the Helmholtz model equation using the time-domain TLM algorithm in the CW regime.

This effect is illustrated in Fig. 4 for a $\kappa = 0.01$ soliton that corresponds to a FWHM width of $w_{\text{FWHM}} \simeq 2\lambda$. In this and all the following figures the x and z axes have equal scalings to permit an easy identification of the beam sizes in terms of the optical wavelength. Figure 4(a) shows the evolution of a linearly diffracting beam with a “sech” shape at its waist. Figure 4(b) shows the fundamental frequency component of a sech beam in a nonlinear medium with the exact input power required for the generation of an exact soliton. The generation of the third harmonic signal, shown in Fig. 4(c), acts as a loss mechanism that arrests the formation of the soliton. Similarly, FWM effects can be noticeable even for wider beams if the total propagation distance is sufficiently large.

THG can be controlled to some extent if the numerical dispersion is enhanced by increasing the step size.^{19,21} Also, one could adjust the numerical frequency cut-off due to the discrete TLM mesh to completely avoid the FWM up-conversion. But any of these strategies assumes a trade-off between the control of the perturbation due to the THG and the numerical accuracy of the calculations. Better strategies can be based on the intentional modelling of typical physical propagation effects that quench THG. For instance, an arbitrary dispersive response can be intentionally introduced in the model.³³ Also, the perturbation due to FWM effects can be avoided assuming a slow nonlinear response, such that the nonlinear refractive index responds to the average optical field $n_{\text{NL}}^2 = \alpha' \langle E_z(x, z, t)^2 \rangle$, where the brackets denote time averaging and only the contribution from the field at the fundamental frequency ω_0 is assumed.^b The continuous wave solution described by

^bThe assumption $n_{\text{NL}}^2 = 2n_0n_2|\tilde{E}|^2$ used in the derivation of the NLH equation corresponds, actually, to $n_{\text{NL}}^2 = \alpha' \langle E_z(x, z, t)^2 \rangle$ and not to $n_{\text{NL}}^2 = \alpha E_z(x, z, t)^2$.

Time Domain Analysis of Helmholtz Soliton Propagation

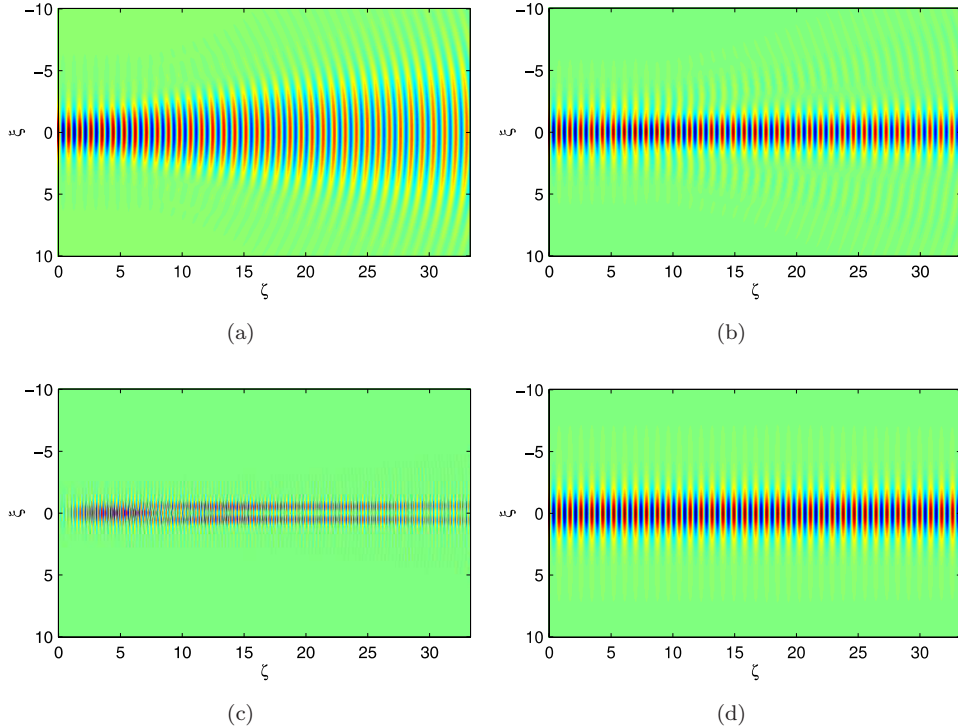


Fig. 4. (a) Linear propagation of a “sech” (at its waist) beam of FWHM width $w_{\text{FWHM}} \simeq 2\lambda$ ($\kappa = 0.01$). (b) Field component at the fundamental frequency ω_0 when the input condition corresponds to the exact soliton (2.11) and an instantaneous nonlinearity is assumed. (c) Third harmonic component. (d) Exact soliton generated in a slow response medium.

the nonlinear Helmholtz equation is then obtained through a transient that depends on the medium response time that can be used as a control parameter. Figure 4(d) shows the exact soliton solution obtained once the THG effect has been eliminated.^c

4.1. Interfaces

The interaction of optical solitons with nonlinear interfaces is a quintessential problem of the Helmholtz nonparaxial type with a fruitful recent progress abundant in new results.^{15–18} The 2D TLM method can extend the numerical surveys to new problems with large variations in the linear and/or nonlinear refractive indexes across the interface which are adequately described by the Helmholtz theory but are out of reach of the NBPM method.⁷

Figure 5 shows the behavior of a Helmholtz soliton with $\kappa = 0.001$ corresponding to $w_{\text{FWHM}} \simeq 6\lambda$ impinging on the planar boundary separating two nonlinear media with an incident angle of $\theta = 45^\circ$. The nonlinear susceptibility $\chi_{\text{NL}}^{(3)}$ is identical

^cNotice that this power is different for the instantaneous and slow response cases when $\alpha = \alpha'$.

P. Chamorro-Posada & G. S. McDonald

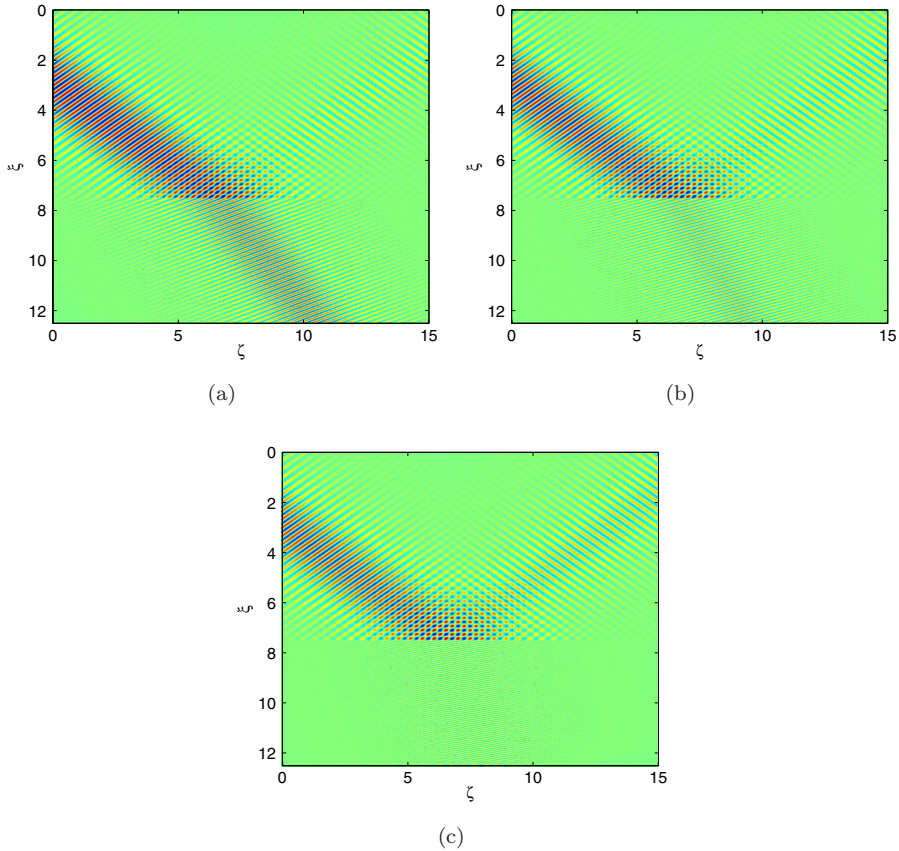


Fig. 5. A $\kappa = 0.001$ soliton ($w_{\text{FWHM}} \simeq 6\lambda$) impinging at 45° on the plane boundary separating two nonlinear media with (a) $\Delta n_L = 0.5$ and (b) $\Delta n_L = 1$ and (c) $\Delta n_L = 1.5$. The nonlinear susceptibility $\chi_{\text{NL}}^{(3)}$ has equal values at both sides of the interface.

at both sides of the discontinuity and the step in the linear refractive index is $\Delta n_L = 0.5$ in Fig. 5(a), $\Delta n_L = 1$ in Fig. 5(b) and $\Delta n_L = 2$ in Fig. 5(c).

4.2. Subwavelength solitons

Electromagnetic propagation in 2D media can be handled using Maxwell equations but it is not possible for the exact physical implementation of a 2D propagation setup. Typically, quasi-two-dimensionality is subject to certain approximations that may fail out of certain parameter regions. Here, we are simply concerned with the relation between the 2D Maxwell equations and the nonlinear scalar Helmholtz equation and its soliton solutions regardless of their possible physical meaning in extreme parameter regimes.

As it was mentioned before, high-intensity subwavelength solitons are proper solutions of the scalar wave equation and were discussed in Ref. 22. In Ref. 23 it

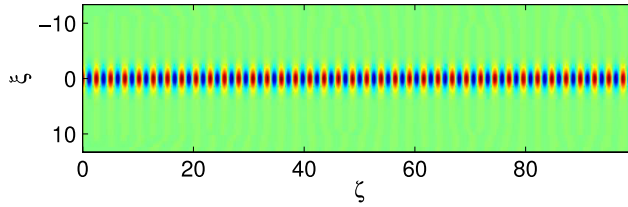


Fig. 6. A subwavelength spatial soliton with $\kappa = 0.1$, $w_{\text{FWHM}} \simeq 0.6 \lambda$.

was argued that such solitons are intrinsically unstable due to the elliptic nature of the evolution equation. In fact, the instability described in Ref. 23 is a purely *numerical* issue and not a physical effect. This numerical instability was studied in detail in Ref. 7, where it is adequately removed from the proposed numerical propagation scheme.

The propagation of a subwavelength spatial soliton as a solution of the time-domain Maxwell equations using the TLM method far beyond the stability limit predicted in Ref. 23 is shown in Fig. 6. The nonparaxiality parameter is $\kappa = 0.1$ that corresponds to a beam width of $w_{\text{FWHM}} = 0.6 \lambda$. Even though subwavelength solitons are free from the intrinsic instability described in Ref. 23, the robustness of these solutions of the nonlinear Helmholtz equation will be the subject of future investigations using the TLM method.

5. Conclusion

We have used a parallel implementation of a nonlinear shunt 2D TLM method for the analysis of the propagation properties of the soliton solutions of the scalar nonlinear Helmholtz equation. We have shown that this scheme permits to extend previous numerical studies to parameter regions that involve relative changes of the (linear or nonlinear) refractive index of $O(1)$. Two particular cases have been considered: spatial solitons at planar interfaces with large contrast in the linear refractive index and the propagation of subwavelength Helmholtz solitons. We have shown that relevant perturbation effects may be originated from nonlinear parametric processes taking place in the computational mesh and how these disturbances can be eliminated.

Acknowledgments

This work has been funded by the Spanish Ministerio de Educación y Ciencia Grant No. TEC2010-21303-C04-04 and Junta de Castilla y León, Grant VA300A12-1.

References

1. S. Trillo and W. Torruellas (eds.), *Spatial Solitons*, *Springer Series in Optical Sciences* (Springer-Verlag, 2010).

P. Chamorro-Posada & G. S. McDonald

2. Y. S. Kivshar and G. P. Agrawal, *Optical Solitons: From Fibers to Photonic Crystals* (Academic Press, London, 2003).
3. T. R. Taha and M. J. Ablowitz, Analytical and numerical aspects of certain nonlinear evolution equations, II. numerical, nonlinear Schrödinger equation, *J. Comput. Phys.* **55**(2) (1984) 203.
4. P. Chamorro-Posada, G. S. McDonald and G. H. C. New, Nonparaxial solitons, *J. Mod. Opt.* **45**(6) (1998) 1111.
5. P. Chamorro-Posada, G. S. McDonald and G. H. C. New, Propagation properties of nonparaxial solitons, *J. Mod. Opt.* **47**(11) (2000) 1877.
6. P. Chamorro-Posada, G. S. McDonald and G. H. C. New, Exact soliton solutions of the nonlinear Helmholtz equation: Communication, *J. Opt. Soc. Am. B* **19** (2002) 1216.
7. P. Chamorro-Posada, G. S. McDonald and G. H. C. New, Nonparaxial beam propagation methods, *Opt. Commun.* **192** (2001) 1.
8. P. Chamorro-Posada and G. S. McDonald, Spatial Kerr soliton collisions at arbitrary angles, *Phys. Rev. E* **74** (2006) 36609.
9. J. M. Christian, G. S. McDonald and P. Chamorro-Posada, Helmholtz solitons in optical materials with a dual power-law nonlinearity, *J. Nonlinear Opt. Phys. Mat.* **19**(3) (2010) 389.
10. J. M. Christian, G. S. McDonald and P. Chamorro-Posada, Helmholtz algebraic solitons, *J. Phys. A, Math. Theor.* **43**(8) (2009) 085212.
11. J. M. Christian, G. S. McDonald and P. Chamorro-Posada, Bistable Helmholtz bright solitons in saturable materials, *J. Opt. Soc. Am B* **26**(12) (2009) 2302.
12. J. M. Christian, G. S. McDonald and R. J. Potton and P. Chamorro-Posada, Helmholtz solitons in power-law optical materials, *Phys. Rev. A* **76**(3) (2007) 033834.
13. J. M. Christian, G. S. McDonald and P. Chamorro-Posada, Bistable Helmholtz solitons in cubic-quintic materials, *Phys. Rev. A* **76**(3) (2007) 033833.
14. J. M. Christian, G. S. McDonald and P. Chamorro-Posada, Helmholtz bright and boundary solitons, *J. Phys. A, Math. Theor.* **40**(7) (2007) 1545.
15. J. Sánchez-Curto, P. Chamorro-Posada and G. S. McDonald, Giant Goos-Hanchen shifts and radiation-induced trapping of Helmholtz solitons at nonlinear interfaces, *Opt. Lett.* **36**(18) (2011) 3605.
16. J. Sánchez-Curto, P. Chamorro-Posada and G. S. McDonald, Helmholtz bright and black soliton splitting at nonlinear interfaces, *Phys. Rev. A* **85**(1) (2012) 013836.
17. J. Sánchez-Curto, P. Chamorro-Posada and G. S. McDonald, Nonlinear interfaces: Intrinsically nonparaxial regimes and effects, *J. Opt. A, Pure Appl. Opt.* **11**(5) (2009) 054015.
18. J. Sánchez-Curto, P. Chamorro-Posada and G. S. McDonald, Helmholtz solitons at nonlinear interfaces, *Opt. Lett.* **32**(9) (2007) 1126.
19. P. B. Johns and R. L. Beurle, Numerical solution of two-dimensional scattering problems using a transmission-line matrix, *Proc. IEE* **118**(9) (1971) 1203.
20. W. J. R. Hofer, The transmission-line matrix method — Theory and applications, *IEEE Trans. Microwave Theory Tech.* **MTT-33**(10) (1985) 882.
21. C. Christopoulos, *The Transmission-line Matrix Method: TLM* (IEEE Press, Piscataway, NJ, 1995).
22. C. Chen and S. Chi, Subwavelength spatial solitons of the TE mode, *Opt. Commun.* **157** (1998) 170.
23. E. Granot, S. Sternklar, Y. Isbi, B. Malomed and A. Lewis, On the existence of subwavelength spatial solitons, *Opt. Commun.* **178** (2000) 431.

Time Domain Analysis of Helmholtz Soliton Propagation

24. P. M. Goorjian and Y. Silberberg, Numericalsimulations of light bullets using the full-vector time-dependent nonlinear Maxwell equations, *J. Opt. Soc. Am. B* **14**(11) (1997) 3253.
25. R. M. Joseph and A. Taflove, Spatial soliton deflection mechanism indicated by FD-TD Maxwell's equations modeling, *IEEE Photon. Technol. Lett.* **6**(10) (1994) 1251.
26. A. D. Boardam, L. Velasco, Y. Papoport and N. King, Ultra-narrow bright spatial solitons interacting with left-handed surfaces, *J. Opt. Soc. Am. B* **22**(7) (2005) 1443.
27. R. M. Joseph, P. M. Goorjian and A. Taflove, Direct time integration of Maxwell's equations in two-dimensional dielectric waveguides for propagation and scattering of femtosecond electromagnetic solitons, *Opt. Lett.* **18**(7) (1993) 491.
28. P. Chamorro-Posada, TLM analysis of multimode interference devices, *Fiber Integrated Opt.* **25**(1) (2006) 1.
29. P. B. Johns and M. O'Brien, Use of the transmission line modeling (T.L.M.) method to solve nonlinear lumped networks, *Radio Electron. Eng.* **50**(1&2) (1980) 59.
30. L. A. Newcombe and J. E. Sitch, Reactive nonlinearities in transmission-line models, *IEE Proc.-A* **132**(2) (1985) 95.
31. S. Y. R. Hui and C. Christopoulos, Discrete transform technique for solving nonlinear circuits and equations, *IEE Proc.-A* **139**(6) (1992) 321.
32. P. Russer, P. P. M. So and W. J. R. Hoefer, Modeling of nonlinear active regions in TLM, *IEEE Microwave Guided Wave Lett.* **1**(1) (1991) 10.
33. L. R. A. X. Menezes and W. J. R. Hoefer, Modeling of general constitutive relationships in SCN TLM, *IEEE Trans. Microwave Theory Tech.* **44**(6) (1996) 854.
34. J. Paul, C. Christopoulos and D. W. P. Thomas, Generalized material models in TLM — part 3: Materials with nonlinear properties, *IEEE Trans. Antennas Propagat.* **50**(7) (2002) 997.
35. V. Janyani, J. D. Paul, A. Vukovic, T. M. Benson and P. Sewell, TLM modelling of nonlinear optical effects in fibre Bragg gratings, *IEE Proc.-J.* **151**(4) (2004) 185.